Investigation of Rotor-Stator Interaction in Turbomachinery

Mathias Legrand, Christophe Pierre, Bernard Peseux

The 10-th of International Symposium on Transport Phenomena and Dynamics of Rotating Machinery
Honolulu, Hawaii, March 07-11, 2004

Paper #044

INVESTIGATION OF ROTOR-STATOR INTERACTIONS IN TURBOMACHINERY

Mathias Legrand
École Centrale de Nantes
Graduate Student
Laboratoire de Mécanique et Matériaux
École Centrale de Nantes
1, rue de la Noë BP 92101
44321 Nantes Cedex 3, France
Phone: +33 2 40 37 25 79
Email: mathias.legrand@ec-nantes.fr

Christophe Pierre
University of Michigan
Stephen P. Timoshenko Collegiate Professor of Mechanical Engineering
Department of Mechanical Engineering,
University of Michigan
3112 G.G. Brown Building
Ann Arbor, MI 48109-2125, USA
Phone: (734) 936 0401
Email: pierre@umich.edu

Bernard Peseux
École Centrale de Nante *Professor of Mechanical Engineering*
Laboratoire de Mécanique et Matériaux
École Centrale de Nantes
1, rue de la Noë BP 92101
44321 Nantes Cedex 3, France
Phone: +33 2 40 37 25 03
Email: bernard.peseux@ec-nantes.fr

ABSTRACT

In modern turbo machines such as aircraft jet engines, contact between the casing and bladed disks may occur through a variety of mechanisms: coincidence of vibration modes, thermal deformation of the casing, rotor imbalance, etc. These nonlinear interactions may result in severe damage to both structures and it is important to understand the physical mechanisms that cause them and under what circumstances they occur. In this study, we focus on the phenomenon of interaction caused by modal coincidence. Simple two-dimensional models of the casing and bladed disk structures are introduced in order to predict the occurrence of contact and the rotation speeds at which response becomes dangerous. Each structure is represented in terms of its two n_d-nodal diameter vibration modes, which are characteristic of axi-symmetric structures and allow for travelling wave motion. These two pairs of nodal diameter modes are made to interact through direct contact and the equations of motion are solved using an explicit time integration scheme in conjunction with the Lagrange multiplier method on the one hand. On the other hand, the Harmonic Balance Method is used for a better understanding of the solutions found by the time integration method. Both methods generally agree well and exhibit two distinct zones of completely different behaviors of the system.

INTRODUCTION

One of the main objectives of turbo-machines engineering is to increase the efficiency of the machines safely. This efficiency, simply defined as the ratio of energy output to energy input, depends strongly on the clearance between the rotating and stationary parts: the wider the clearance, the less efficient the machine. The shapes optimization and the reduction of the clearance are critical because they increase the possibility of contact between both structures. This contact has many origins: gyroscopic effect under certain operating conditions, apparition of a rotor imbalance due to the uncertainties of the design or following bird ingestions. After this type of contact, several different dynamic phenomena could appear: forced excitation of the modeshapes of a blade resulting in the fragmentation of the tip of this latter or coupling between the vibration modes of the casing and those of the bladed disk, generally called "modal interaction": to the best of our knowledge, one particularly interesting relevant dissertation by Schmiechen (1997) and a paper by Legrand *et al.* (2003) deal with this travelling wave speed coincidence. In none of the other literature on the topic is there any consideration of the interaction between two flexible structures in contact.

The primary goal of the present paper is to give a better understanding of the modal interaction between the stator and the rotor in a jet-engine. This non linear interaction may lead to devastating effects like the destruction of the engine and jeopardizes passengers' safety. It is therefore important to get a full insight of the phenomenon and to give accurate predictions. To this end, a simple numerical tool, based on two elastic structures discretized on their own modeshapes has been developed. Each structure is represented in terms of its two n_d-nodal diameter vibration modes which allow for travelling wave motion. The kinetic energy of the rotor is transformed into vibratory energy thanks to direct contact between the two structures and may result in a case of interaction.

The paper is organized as follows. In the first section, very simple mathematical statements explain the concept of modal interaction. Then, in the second section, the modelization of the structures used in the numerical tool is presented. The interaction is investigated by an explicit time integration method, in a third part, and by the Harmonic Balance Method in a fourth section. This method has shown very promising results for strong non linearities (Poudou and Pierre (2002)). Finally, the new results found are explained.

1 MODAL INTERACTION DEFINITION

The axi-symmetry of a structure, like a bladed disk or a casing, which mathematically leads to circulant mass and stiffness matrices, gives rise to mode pairs with identical natural frequencies,

except for zero nodal diameter modes with a simple natural frequency as explained by Bladh (2000). Both respective mode-shapes are similar and rotated around the axis of symmetry by $\pi/(2n_d)$ where n_d is the number of nodal diameters. In that special case, it is possible to combine these two modes into forward and backward travelling waves. Assuming that θ represents an angular position and α, an amplitude of deflection, these two rotating waves are expressed as:

$$\begin{aligned}\alpha_f(t,\theta) &= \alpha_0 \cos(\omega t - n_d(\theta - \theta_0)) \\ \alpha_b(t,\theta) &= \alpha_0 \cos(\omega t + n_d(\theta - \theta_0))\end{aligned} \tag{1}$$

where ω is the pulsation and θ_0 an undetermined parameter of angular position. For a static structure, the propagation velocity of these two waves in a stationary frame is $\pm\omega/n_d$, considering the direction of rotation. For a rotating structure like a bladed disk in a turbo-machine, the angular rotational velocity Ω (positive in a counter-clockwise direction) has to be added. The propagation velocity of these two waves in a stationary frame becomes then $\Omega + \omega/n_d$ for the forward rotating wave and $\Omega - \omega/n_d$ for the backward rotating wave. If both structures vibrate at their own natural frequencies, denoted ω_c for the casing and ω_{bd} for the bladed disk, four cases of travelling wave speed coincidence can be stated for Ω:

$$\pm\omega_c = n_d\Omega \pm \omega_{bd} \tag{2}$$

Taking into account physical considerations on the direction of the contact force between the two structures - forward on the casing and backward on the bladed disk if the rotor rotates counter-clockwise -, only one of these equations can be considered as dangerous:

$$\omega_c = n_d\Omega - \omega_{bd} \tag{3}$$

At this speed, both structures are driven in resonance by the contact forces. This rotational speed must be avoided because resonance can cause undesired large amplitude vibrations.

2 MODELIZATION OF THE STRUCTURES

2.1 BLADED DISK

For this study, the bladed disk is modelled as simply as possible. A given number N_b of rigid bodies linked to the disk and between each other by a stiffness constitutes the rotating structure. The structure is depicted in Fig. 1. The stiffening due to centrifugal forces is neglected in this model. The equation associated to the

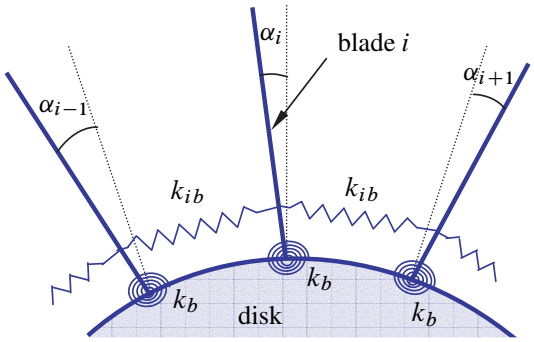

Fig. 1: Schematic of the bladed disk

ith blade (or rigid body) is:

$$m_b\ddot{\alpha}_i + (k_b + 2k_{ib})\alpha_i - k_{ib}(\alpha_{i+1} + \alpha_{i-1}) = 0 \tag{4}$$

where α_i represents the vibration angle of the ith blade. This equation becomes, when generalized to the entire structure:

$$\mathbf{M_{bd}}\ddot{\boldsymbol{\alpha}} + \mathbf{K_{bd}}\boldsymbol{\alpha} = \mathbf{0} \tag{5}$$

The mass matrix contains the moment of inertia of a rigid beam about one of its ends m_b on its diagonal:

$$\mathbf{M_{bd}} = \begin{bmatrix} m_b & 0 & \dots & 0 \\ 0 & \ddots & \ddots & \vdots \\ \vdots & \ddots & \ddots & 0 \\ 0 & \dots & 0 & m_b \end{bmatrix} \tag{6}$$

Noting $k_1 = k_b + 2k_{ib}$ and $k_2 = -k_{ib}$ the circulant stiffness matrix becomes:

$$\mathbf{K_{bd}} = \begin{bmatrix} k_1 & k_2 & 0 & \dots & 0 & k_2 \\ k_2 & k_1 & k_2 & 0 & \dots & 0 \\ 0 & & \ddots & & & \vdots \\ \vdots & & & \ddots & & 0 \\ 0 & \dots & 0 & k_2 & k_1 & k_2 \\ k_2 & 0 & \dots & 0 & k_2 & k_1 \end{bmatrix} \tag{7}$$

The eigenshapes of the bladed disk are calculated from this model. Their two n_d-nodal diameter modal contributions are denoted α_c and α_s.

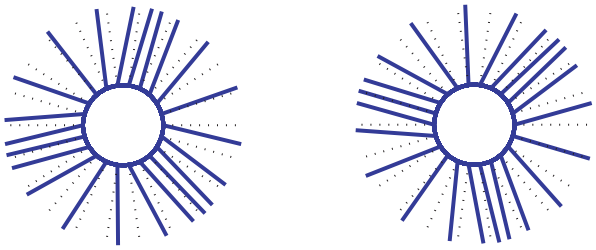

Fig. 2: 3-nodal diameter modes of the bladed disk

2.2 CASING

The casing is directly discretized in the modal coordinates by keeping only its two n_d-nodal diameter modes (Fig . 3). Their contributions are denoted u_c and u_s.During the calculations, structural damping is added in the equations for both structures.

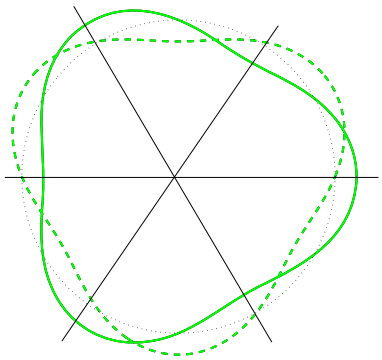

Fig. 3: Discretization of the casing on its 3-nodal diameter modes

3 CONTACT EQUATIONS AND TIME INTEGRATION

3.1 THEORY

The forces of particular interest in this study are the forces of contact acting between the blade tips and the casing. No friction is considered. The model is thus conservative and Hamilton's Principle can be used for the derivation of the equations. The so-called impenetrability condition is enforced by the Lagrange multiplier method. Due to the chosen configuration space, this method has no physical interpretation and may be viewed as a simple mathematical correction of the displacements of the structures in order to avoid any penetration between them. Hamilton's Principle is written as follows:

$$\int_{t_1}^{t_2} \delta T - \delta U + \delta E_{cont} dt = 0 \quad \forall(\delta\boldsymbol{\alpha}, \delta\mathbf{u}, \delta\boldsymbol{\lambda}) \tag{8}$$

satisfying $\delta\boldsymbol{\alpha}(t_1) = \delta\boldsymbol{\alpha}(t_2) = \delta\mathbf{u}(t_1) = \delta\mathbf{u}(t_2) = 0$. The different energies take the forms:

$$T = \frac{1}{2}\dot{\mathbf{u}}^T \mathbf{M_c} \dot{\mathbf{u}} + \frac{1}{2}\dot{\boldsymbol{\alpha}}^T \mathbf{M_{bd}} \dot{\boldsymbol{\alpha}}$$

$$U = \frac{1}{2}\mathbf{u}^T \mathbf{K_c} \mathbf{u} + \frac{1}{2}\boldsymbol{\alpha}^T \mathbf{K_{bd}} \boldsymbol{\alpha}$$

$$E_{cont} = \boldsymbol{\lambda}^T \mathbf{g}(\mathbf{u}, \boldsymbol{\alpha})$$

where $\mathbf{u}$ and $\boldsymbol{\alpha}$ are the displacement vectors of the casing and the bladed disk, respectively. $\boldsymbol{\lambda}$ and $\mathbf{g}$ contain the Lagrange multipliers and the gap functions between the blade tips and the casing. This formulation is discretized in time using the explicit central differences scheme. Denoting the displacement vector of the two structures by $\mathbf{x}$, one has:

$$\begin{cases} \ddot{\mathbf{x}}_n = \dfrac{\mathbf{x}_{n+1} - 2\,\mathbf{x}_n + \mathbf{x}_{n-1}}{h^2} \\ \dot{\mathbf{x}}_n = \dfrac{\mathbf{x}_n - \mathbf{x}_{n-1}}{h} \end{cases} \tag{9}$$

This scheme is stable for a very small time step h bounded by the Courant Criterion in linear cases. The velocity vector $\dot{\mathbf{x}}_n$ is approximated this way to guarantee the robustness of the following algorithm.

3.2 ALGORITHM

Carpenter *et al.* (1991) explained that an explicit time integration scheme in conjunction with the Lagrange multiplier method dealing with contact problems is generally divided into three steps and is fairly simple:

1. prediction of the displacements without considering any possible contact.
2. determination of the penetrations between the structures.
3. correction of the displacements through the calculation of the Lagrange multipliers in order to eliminate all the penetrations.

The time step size allows for the linearization of the equations with respect to time between the prediction and the correction steps. The algorithm becomes:

prediction The displacements of both structures are calculated in modal coordinates. It yields the prediction of four unknowns u_c^*, u_s^*, α_c^* and α_s^*. The superscript * means that the unknowns are only predicted during the time step $n+1$.

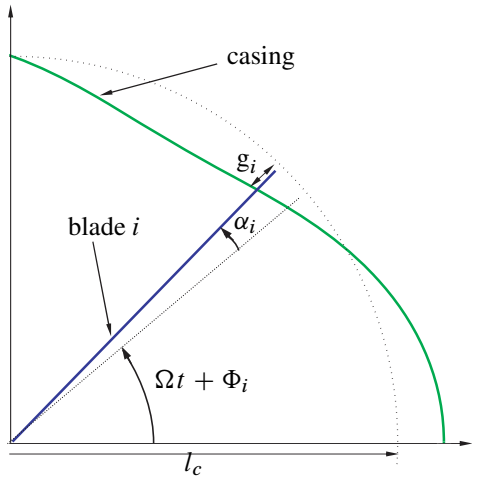

Fig. 4: Schematic of the gap function g_i

determination of the gap functions The angle of each blade is deduced from the modal prediction by a projection onto the physical coordinates:

$$\begin{Bmatrix} \alpha_1^* \\ \alpha_2^* \\ \vdots \\ \alpha_{N_b-1}^* \\ \alpha_{N_b}^* \end{Bmatrix} = \begin{bmatrix} & \\ \mathbf{p_1} & \mathbf{p_2} \\ & \end{bmatrix} \cdot \begin{Bmatrix} \alpha_c^* \\ \alpha_s^* \end{Bmatrix} \tag{10}$$

$\mathbf{p_1}$ and $\mathbf{p_2}$ are the two n_d-nodal diameter modes of the bladed disk. For each blade i, a new angle is defined: $\beta_i = n_d\theta_i$ with $\theta_i = \Omega t + \Phi_i + \alpha_i$. The gap function is then given by:

$$g_i = l_c - l_a + u_c^* \cos(\beta_i^*) + u_s^* \sin(\beta_i^*) \tag{11}$$

where l_a is the length of a blade, l_c, the radius of the casing and Φ_i the initial angle of the ith blade in a stationary frame.

correction of the displacements Lagrange multipliers have to be calculated such as nulling the gap between the guessed penetrating blades and the casing. Due to the linearization explained above, this correction consists in the resolution of a $(2N+2)\cdot(2N+2)$ linear system where N is the number of blades in contact with the casing during the on-going time step. An example of the linear system is given for a case with two blades in contact, the first and fourth ones:

$$\mathbf{K_C} = \begin{bmatrix} m_c & 0 & 0 & 0 & \cos\beta_1^* & \cos\beta_4^* \\ 0 & m_c & 0 & 0 & \sin\beta_1^* & \sin\beta_4^* \\ 0 & 0 & m_{bd} & 0 & A_1^* & 0 \\ 0 & 0 & 0 & m_{bd} & 0 & A_4^* \\ \cos\beta_1^* & \sin\beta_1^* & A_1^* & 0 & 0 & 0 \\ \cos\beta_4^* & \sin\beta_4^* & 0 & A_4^* & 0 & 0 \end{bmatrix}$$

$$\mathbf{U_C} = \begin{Bmatrix} u_c^{n+1} - u_c^* \\ u_s^{n+1} - u_s^* \\ \alpha_1^{n+1} - \alpha_1^* \\ \alpha_4^{n+1} - \alpha_4^* \\ \lambda_1 \\ \lambda_4 \end{Bmatrix}, \quad \mathbf{F_C} = \begin{Bmatrix} 0 \\ 0 \\ 0 \\ 0 \\ -g_1 \\ -g_4 \end{Bmatrix}$$

where $A_i^* = n_d(-u_c^* \sin\beta_i^* + u_s^* \cos\beta_i^*)$. $\mathbf{U_C}$ is unknown and is calculated by inverting the system $\mathbf{K_C} \cdot \mathbf{U_C} = \mathbf{F_C}$. The correction for the bladed disk is carried out in the physical coordinates and is projected onto the modal coordinates. Finally, time is incremented and a new prediction is calculated.

3.3 RESULTS

In this section, we present some numerical results illustrating the behavior of the mechanical system previously presented due to the contact between the rotor and the stator initiated by a very short forcing pulse of fifty time steps (50μs) on the first mode u_c of the casing at the very beginning of the simulation. For sake of simplicity, the rotor is constituted of eight blades and both structures are discretized on their two three-nodal diameter modes. It has to be noted that the rotor of the chosen model is perfectly balanced and no eccentricity between the two structures is introduced.

3.3.1 VALIDATION

The validation of the algorithm has been carried out in two different ways. First, a convergence study of the time step has shown that $h = 10^{-6}$s is sufficient to get significant results while minimizing computational efforts. Next, a focus on the distances between the blade tips and the casing depicted in Fig. 5 confirms that the contact algorithm is successful for the chosen time step: the gap distance never becomes negative and the algorithm remains stable for all times. It is interesting to note the accuracy of the contact-algorithm based on a four-degrees of freedom model.

3.3.2 RESPONSE OF THE STRUCTURES

Browsing the space of initial conditions, two main types of responses appear. The first one is characterized by several impacts between the two structures, followed by a decrease of the amplitudes of vibration to zero due to structural damping. This response is not of interest. In contrast, an exchange of energy between the stator and the rotor occurs in the second type of responses. This interesting case features, after the transient response, a steady state where several blades remain in permanent contact with the casing without vibrating, while the other blades do not impact the casing anymore. Solid and dashed bold black lines in Fig. 5 show the two blades in permanent contact for a numerical simulation of an 8-bladed disk interacting with the casing. The propagation of the deformation wave of the casing has the same angular velocity as the bladed disk, and the latter reaches a permanent static-only deformation state as observed in Fig. 6. This new phenomenon is referred to as locked motion and is studied in details in what follows.

3.3.3 CONDITIONS OF INTERACTION

It appears that several parameters (rotational velocity of the rotor, initial impact amplitude, structural damping...) and the combi-

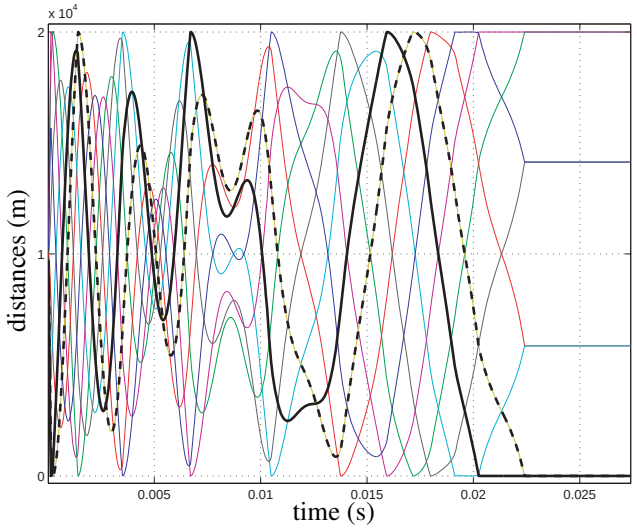

Fig. 5: Distances between the casing and the blade tips

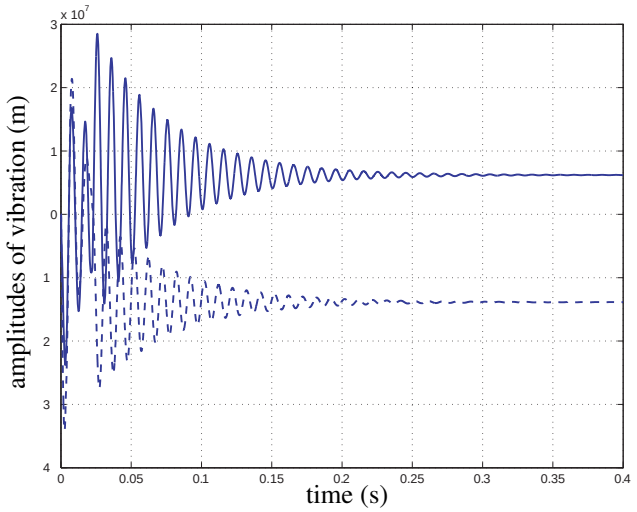

Fig. 6: Modal vibrations of the bladed disk versus time

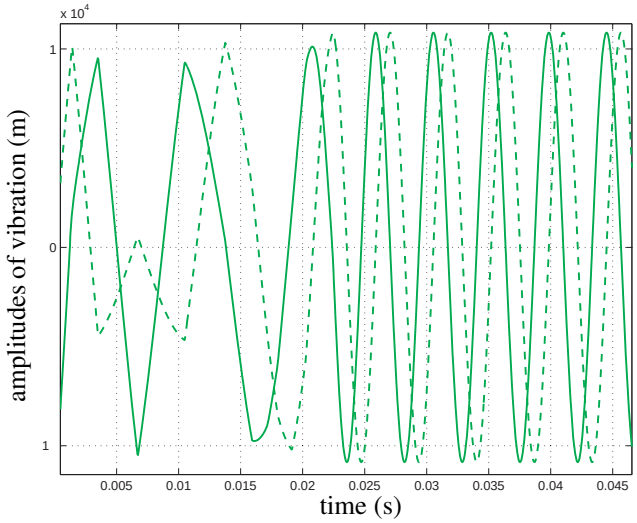

Fig. 7: Modal vibrations of the casing versus time

nation thereof play a key role on the occurrence of locked motion. Concerning the rotational velocity and the initial forcing pulse amplitude, Fig. 8 shows a zone of possible interaction for $\Omega \geq \omega_c/n_d$. The initial forcing pulse in this zone must be suffi-

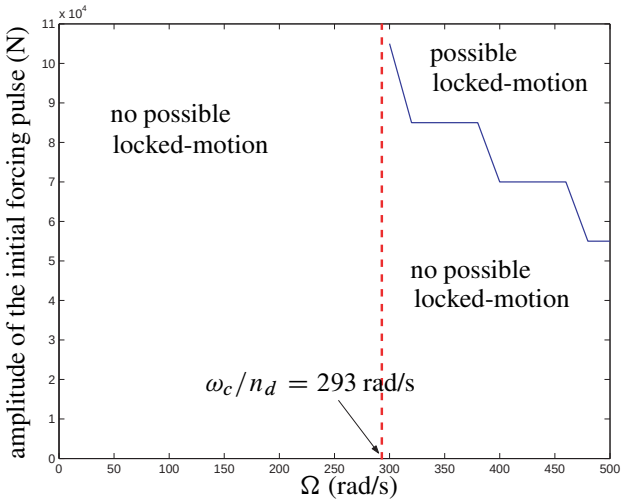

Fig. 8: Zone of possible interaction in the rotational velocity-amplitude of the initial forcing pulse space

ciently large to make the interaction phenomenon appear. Below ω_c/n_d whatever the initial conditions, the locked motion is impossible. A deeper study taking into account the structural damping of the casing and the bladed disk is rendered difficult because of the addition of two new parameters. Then, a clear conclusion on the time integration results is early and a new approach is used and explained in section four. Although the few previous findings have shown the importance of the natural frequency of the bladed disk ω_{bd} (see Eq. 3), Fig. 6 demonstrates that the role of this structure in the phenomenon vanishes because of its permanent static-only deformation state behavior during the interaction.

3.3.4 STABILITY OF THE "LOCKED-MOTION"

After the locked motion is reached, a new forcing pulse of fifty time steps is applied on the first mode u_c of the casing. For a very high amplitude of this pulse, the motion jumps from a locked motion 1 to a locked motion 2 instantaneously. Even if the blades in permanent contact are different, their number remains the same. The motion is then stable in amplitude but is able to take many states as illustrated in Fig. 9 where the red arrows indicate the blades in permanent contact before and after the forcing pulse.

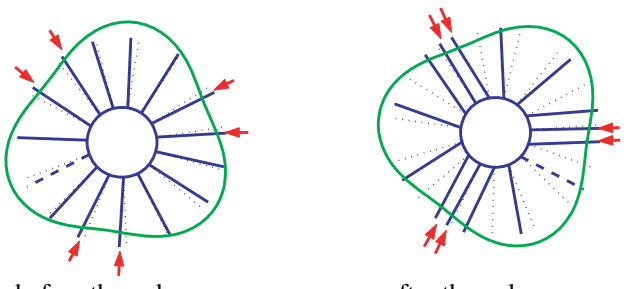

Fig. 9: States of the two structures before and after the second forcing pulse

4 FREQUENCY-DOMAIN STUDY OF THE "LOCKED MOTION"

In order to avoid the high sensitivity of the results to initial conditions, and particularly to the amplitude of the initial forcing pulse, the method of Harmonic Balance (HB) is used. This frequency-domain method is capable of predicting efficiently the steady state periodic behavior of nonlinear mechanical systems without considering the initial conditions (Pierre *et al.* (1985)). The HB method also allows for parametric studies that would be carry prohibitive cost using direct time integration, and results in a better physical understanding of the solutions.

4.1 GOVERNING EQUATIONS

The time integration model is kept in this section. The two blades in permanent contact with the casing are denoted by i_1 and i_2. The resulting equations are:

- for the casing

$$\begin{cases} m_c\,\ddot{u}_c + k_c\,u_c + \sum_{j=1}^{2} \lambda_j \cos\beta_{i_j} = 0 \\ m_c\,\ddot{u}_s + k_c\,u_s + \sum_{j=1}^{2} \lambda_j \sin\beta_{i_j} = 0 \end{cases} \tag{12}$$

- for the two blades in contact

$$\begin{aligned} \forall\, j = 1,2 \quad & (k_a + 2k_b)\alpha_{i_j} - k_b(\alpha_{i_j-1} + \alpha_{i_j+1}) \\ & + \lambda_j n_d(-u_c \sin\beta_{i_j} + u_s \cos\beta_{i_j}) = 0 \end{aligned} \tag{13}$$

- for the remaining blades

$$\begin{cases} (k_a + 2k_b)\alpha_1 - k_b(\alpha_N + \alpha_2) = 0 \\ (k_a + 2k_b)\alpha_i - k_b(\alpha_{i-1} + \alpha_{i+1}) = 0 \\ \quad \forall\, i \in [2, N-1] - \{i_1, i_2\} \\ (k_a + 2k_b)\alpha_N - k_b(\alpha_{N-1} + \alpha_1) = 0 \end{cases} \tag{14}$$

- for blades i_1 and i_2

$$\forall\, j = 1,2 \quad u_c \cos\beta_{i_j} + u_s \sin\beta_{i_j} = l_a - l_c \tag{15}$$

In order to decrease the size of the problem, the bladed disk displacements are written in the modal coordinates. This formulation results in a non linear differential system of six equations and six unknowns $u_c, u_s, \lambda_1, \lambda_2, \alpha_c, \alpha_s$ that cannot be solved analytically.

4.2 SOLUTION METHOD

The HB method is used to find a solution to this non linear differential system for several reasons:

- this approach is a classical technique for studying non linear system oscillations.
- in this method, the response being sought and the non linear restoring forces are expanded in two Fourier series: the time integration has shown almost pure harmonic or static responses

- HBM is not sensitive to the initial conditions which represent a critical issue in the time integration method.
- HBM transforms a non linear differential system of equations in a non linear algebraic system of equations that can be easier to solve.

Observing time integration results, a simple harmonic is kept for the casing:

$$\begin{cases} u_c = u_c^c \cos(n_d \Omega t) + u_c^s \sin(n_d \Omega t) \\ u_s = u_s^c \cos(n_d \Omega t) + u_s^s \sin(n_d \Omega t) \end{cases} \quad (16)$$

The two contact forces and the two bladed disk modal contributions are assumed to be constant. A projection of Eqs 12, 13, 14 and 15 onto $[1, \cos(n_d \Omega t), \sin(n_d \Omega t)]$ basis followed by an integration over the domain $t = [1, 2\pi/(n_d \Omega)]$ (Galerkin method) leads to a non linear algebraic system of eight equations and eight unknowns. The vector solution is obtained iteratively by a non linear algorithm such as the quasi-Newton method of Matlab in our case.

4.3 RESULTS

The previous equations have been solved with Ω as a parameter. All values are Ω-dependent except the vibrations of the casing which are bounded by the initial clearance between the blade tips and the casing in itself. $\Omega = \omega_c/n_d$ seems to be a particular rotational velocity for this system: it is confirmed by modifying the mechanical characteristics of the casing and thus its natural frequency ω_c. The sign of the Lagrange multipliers changes exactly for this value. The solution given by the HB method in Fig. 10 is physically unacceptable for $\Omega < \omega_c/n_d$ though numerically correct. Further simple calculations on the contact forces would show that the casing is pushing the bladed disk for $\Omega < \omega_c/n_d$ which is impossible. This main result is consistent with the pre-supposed interaction zone of the time integration results depicted in Fig. 8: the locked-motion is not reachable for $\Omega \leq \omega_c/n_d$ whatever the initial forcing amplitudes are. The introduction of an engine order

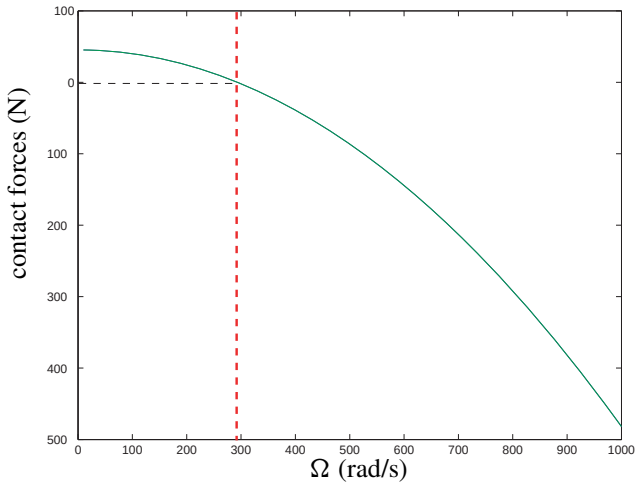

Fig. 10: Amplitudes of the contact forces versus Ω

excitation in the equations has no notable effects on the results for both methods.

CONCLUSION

In this paper, a numerical tool has been developed in order to study the modal interaction between a rotor and a stator in a turbomachine. The model used is based on a exact mathematical formulation of the contact in conjunction with a modal description of the motion. A zone of possible interaction referred to as locked motion in this study, because of the characteristics of its behavior, has been found by both HB and time integration methods. Contrary to previous findings, the bladed disk natural frequency plays no role in the occurrence of the locked motion phenomenon. Moreover, the initial gap between the blade tips and the casing limits the amplitudes of vibration of the casing and forbids any amplitude divergence. In future work, it would be of interest to include a small eccentricity between the structures in order to apply a rotating excitation due to contact on the bladed disk as well as the casing.

REFERENCES

[1] R. Bladh. *Efficient predictions of the vibratory response of mistuned bladed disk by reduced order modeling*. PhD thesis, University of Michigan, 2000.

[2] N. Carpenter, R. Taylor, and M. Katona. Lagrange constraints for transcient finite element surface contact. *International Journal for Numerical Methods in Engineering*, 32:103–128, 1991.

[3] M. Legrand, B. Peseux, and C. Pierre. Amélioration de la prédiction de l'interaction rotor/stator dans un moteur d'avion. In *Sixième Colloque National en Calcul des Structures*, Giens, France, 2003.

[4] C. Pierre, A.A. Ferri, and E.H. Dowell. Multi harmonic analysis of dry friction damped systems using an incremental harmonic balance method. *Journal of Applied Mechanics*, 52:958–964, 1985.

[5] O. Poudou and C. Pierre. Hybrid frequency-time domain methods for the analysis of complex structural systems with dry friction damping. In *Proceedings of the 44-th AIAA/ASME/ASCE/AHS/ASC Structures, Structural Dynamics and Material Comference*, number 2003-1411, Norfolk, Virginia, USA, 2002.

[6] P. Schmiechen. *Travelling Wave Speed Coincidence*. PhD thesis, Imperial College of Science, Technology and Medecine - University of London, 1997.